



Kent Academic Repository

Wang, Junyuan, Gomes, Nathan J. and Wang, Jiangzhou (2018) *Adaptive Frequency Reuse for Beam Allocation Based Multiuser Massive MIMO Systems*. In: 2018 IEEE International Conference on Communications (ICC). IEEE. ISBN 978-1-5386-3181-2.

Downloaded from

<https://kar.kent.ac.uk/68900/> The University of Kent's Academic Repository KAR

The version of record is available from

<https://doi.org/10.1109/ICC.2018.8422264>

This document version

Author's Accepted Manuscript

DOI for this version

Licence for this version

UNSPECIFIED

Additional information

Versions of research works

Versions of Record

If this version is the version of record, it is the same as the published version available on the publisher's web site. Cite as the published version.

Author Accepted Manuscripts

If this document is identified as the Author Accepted Manuscript it is the version after peer review but before type setting, copy editing or publisher branding. Cite as Surname, Initial. (Year) 'Title of article'. To be published in *Title of Journal*, Volume and issue numbers [peer-reviewed accepted version]. Available at: DOI or URL (Accessed: date).

Enquiries

If you have questions about this document contact ResearchSupport@kent.ac.uk. Please include the URL of the record in KAR. If you believe that your, or a third party's rights have been compromised through this document please see our [Take Down policy](https://www.kent.ac.uk/guides/kar-the-kent-academic-repository#policies) (available from <https://www.kent.ac.uk/guides/kar-the-kent-academic-repository#policies>).

Adaptive Frequency Reuse for Beam Allocation Based Multiuser Massive MIMO Systems

Junyuan Wang, Nathan J. Gomes and Jiangzhou Wang

School of Engineering and Digital Arts, University of Kent, Canterbury, Kent, CT2 7NT, United Kingdom

Email: {jw712, n.j.gomes, j.z.wang}@kent.ac.uk

Abstract—Massive multiple-input-multiple-output (MIMO) is a promising technique to provide high-data-rate communication in fifth-generation (5G) mobile systems, thanks to its ability to form narrow and high-gain beams. Among various massive MIMO beamforming techniques, the fixed-beam scheme has attracted considerable attention due to its simplicity. In this paper, we focus on a fixed-beam based multiuser massive MIMO system where each user is served by a beam allocated to it. As the directions of fixed beams are predetermined and the users are randomly distributed, there could be some “worst-case” users, located at the edge of its serving beam, suffering from strong inter-beam interference and thus experiencing low data rate. To improve the individual data rates of the worst-case users while maintaining the sum data rate, an adaptive frequency reuse scheme is proposed. Simulation results corroborate that our proposed adaptive frequency reuse strategy can greatly improve the worst-case users’ data rates without sacrificing the sum data rate.

Index Terms—Adaptive frequency reuse, beam allocation, achievable data rate, worst-case users, massive multiple-input-multiple-output (MIMO)

I. INTRODUCTION

10 support various high-data-rate mobile applications, massive multiple-input-multiple-output (MIMO) has been proposed as a promising technique for the fifth-generation (5G) mobile communication system [1]. In a massive MIMO system, a large number of antennas are deployed at the base-station (BS), thanks to which narrow and high-gain beams can be formed and high spectral efficiency can be achieved [2]–[4].

Despite the great potential of massive MIMO, it is difficult to apply the traditional digital beamforming techniques to a massive MIMO system in practice because one dedicated radio frequency (RF) chain is required for each antenna element, which requires high implementation cost and high energy consumption. To reduce the number of required RF chains in a massive MIMO system, research has been focused on analog beamforming [5]–[8] where a beam is formed by adjusting the independent phase shifters on the BS antennas at the RF part (i.e., only one RF chain is needed for a single data stream), and hybrid analog-digital beamforming [9]–[15].

For both analog and hybrid analog-digital beamforming systems, a fixed-beam network along with beam selection has emerged as a popular technique due to its simplicity [8]–[12]. With fixed-beam techniques, a fixed number of beams are generated to serve the users in the cell, and each selected

beam is connected to a dedicated RF chain. A simple fixed-beam based pure analog beamforming system was considered in [8] where each user is served by an allocated beam. By assuming universal frequency reuse among the beams, a low-complexity beam allocation (LBA) algorithm is proposed in [8] to maximize the sum data rate, which achieves nearly optimal performance. However, as the users are randomly located within the cell and have distinct angular separation from the main direction of their serving beams, there are always users, especially those at a serving beam edge, suffering from low power efficiency and high inter-beam interference, and thus low data rates. Since it is equally important to maximize the sum data rate and reduce the rate disparity of the users, we aim to improve the data rates of these “beam-edge” users, referred to as *worst-case users*, in this paper.

Note that the low data rate of a worst-case user results from the severe inter-beam interference coming from the adjacent beams of its serving beam. To mitigate the inter-beam interference for the worst-case users, we propose to allocate distinct frequency bands for the highly interfered adjacent beams. An adaptive frequency reuse scheme is then proposed to effectively mitigate the strong inter-beam interference while maintaining the sum data rate. Simulation results show that our proposed adaptive frequency reuse scheme can improve the worst-case users’ data rates and achieve similar sum data rate to universal frequency reuse.

The remainder of this paper is organized as follows. Section II introduces the system model. The beam allocation is discussed in Section III, and an adaptive frequency reuse scheme is proposed in Section IV. Conclusions are summarized in Section V.

Throughout this paper, $\mathbb{E}[\cdot]$ denotes the expectation operator. $|X|$ denotes the cardinality of set X . $X \cap Y$ and $X \cup Y$ denote the intersection and union of set X and set Y , respectively. $X \setminus Y$ denotes the relative compliment of set Y in set X . \emptyset denotes the empty set.

II. SYSTEM MODEL

Consider the downlink transmission of a beam allocation based multiuser massive MIMO system as shown in Fig. 1. K users are assumed to be uniformly distributed within a circular cell with unit radius, and each user is equipped with a single antenna. A massive number of N fixed beams are formed by deploying the Butler network [16] with a linear array of N antenna elements at the BS. Denote the set of users as \mathcal{K} and

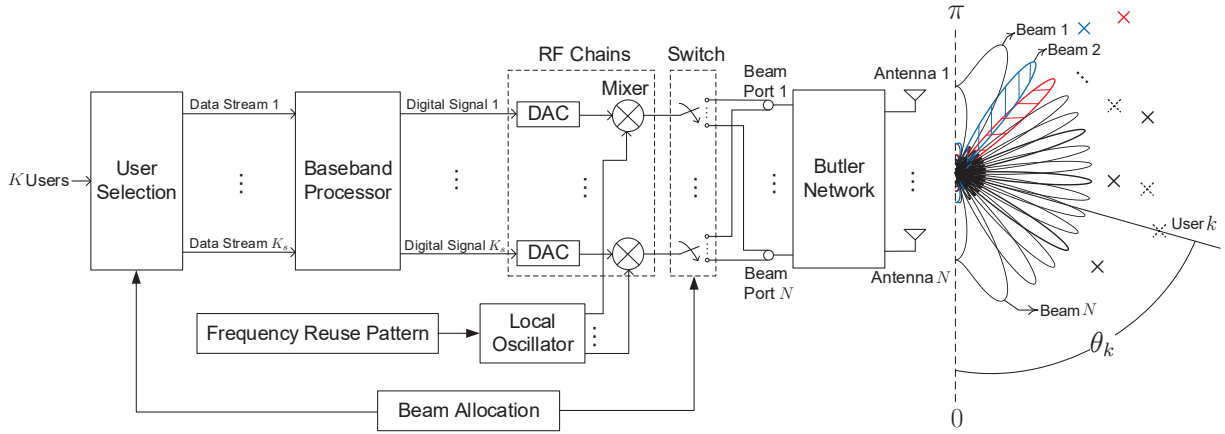


Fig. 1. Illustration of downlink beam allocation based multiuser massive MIMO systems. “x” represents a user. The served users and active beams are plotted in solid lines while the unserved users and inactive beams are plotted in dashed lines. A beam is allocated to the user in the same color where “black” represents that the beams work on the whole frequency band, and “red” and “blue” represent that the beams work on two distinct subbands, respectively.

the set of beams as \mathcal{B} , with $|\mathcal{K}| = K$ and $|\mathcal{B}| = N$. The BS is located at the center of the cell and all the BS antenna elements are equally spaced at half propagation wavelength.

For the beam allocation based system, each user is served by an individual beam allocated to it. Denote the set of served users as \mathcal{K}_s and the corresponding set of serving beams as \mathcal{B}_s with $|\mathcal{K}_s| = |\mathcal{B}_s| = K_s$. As shown in Fig. 1, with the feedback of the beam allocation result, i.e., which beam is allocated to which user for data transmission, K_s out of K users are selected to be served and their K_s corresponding data streams are sent for baseband waveform processing. Then, each digital basedband output signal passes through its own RF chain, and the corresponding RF signal is fed into a particular beam port n via a switch to activate the allocated beam n for its data transmission.

It can be seen from Fig. 1 that the data transmission is determined by the beam allocation and frequency reuse schemes. Specifically, beam allocation determines how to efficiently allocate beams to users for data transmission, which will be discussed in Section III. Frequency reuse pattern determines the working frequency of each active beam. For example, in Fig. 1, the solid black beams are allocated with the whole frequency band as their adjacent interfering beams are off and the inter-beam interference is small. In this case, using the whole frequency band for transmission can achieve higher data rate. For the shaded blue and red beams, two distinct subbands are allocated since their served users are very close to each other, and the cross-interference is strong and needs to be eliminated. Therefore, it is important to design an efficient frequency reuse scheme to mitigate the inter-beam interference, which will be investigated in Section IV.

By applying the Butler network to form N beams where N is a power of 2, the directivity, i.e., beam gain, of any beam $n \in \mathcal{B}$ with respect to the angle θ is given by [8]

$$D_n(\theta) = \frac{\sin^2(0.5N\pi \cos \theta - \beta_n)}{N \sin^2(0.5\pi \cos \theta - \frac{1}{N}\beta_n)}, \quad (1)$$

where

$$\beta_n = \left(-\frac{N+1}{2} + n\right)\pi. \quad (2)$$

By assuming a line-of-sight (LOS) channel at millimeter-wave (mmWave) frequencies, the departure angle of the signal received at user k is θ_k as illustrated in Fig. 1, and the received power of the desired signal can be written as [17]

$$P_k = p_{n_k^{(1)}} \cdot D_{n_k^{(1)}}(\theta_k) \cdot \rho_k^{-\alpha}, \quad (3)$$

where $p_{n_k^{(1)}}$ denotes the transmit power allocated to user k 's serving beam $n_k^{(1)}$. ρ_k is the distance from the cell center to user k and α is the path-loss exponent. Assuming that the total transmit power at the BS is fixed at P_t and equally allocated to all the active beams, the transmit power allocated on beam $n \in \mathcal{B}_s$ is given by

$$p_n = \frac{P_t}{K_s}, \quad (4)$$

where $K_s = |\mathcal{K}_s| = |\mathcal{B}_s|$ is the number of active beams. As the users are served by their allocated beams, beam allocation with universal frequency reuse will be first discussed in the following section.

III. BEAM ALLOCATION UNDER UNIVERSAL FREQUENCY REUSE

With universal frequency reuse, by assuming that the total system bandwidth is normalized to unity, the achievable data rate of user $k \in \mathcal{K}_s$ can be written as

$$R_k^{uni} = \log_2 \left(1 + \frac{P_k}{\sigma_0^2 + I_k^{uni}}\right), \quad (5)$$

where σ_0^2 is the variance of the additive white Gaussian noise (AWGN), and I_k^{uni} is the inter-beam interference power received at user k , given by

$$I_k^{uni} = \sum_{n \in \mathcal{B}_s, n \neq n_k^{(1)}} p_n \cdot D_n(\theta_k) \cdot \rho_k^{-\alpha}. \quad (6)$$

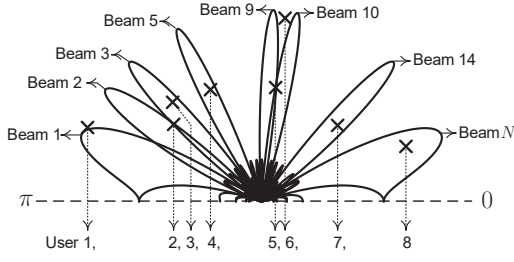


Fig. 2. Illustration of beam allocation result for a random realization of users' positions with LBA algorithm. "x" represents a served user. Only the active beams are drawn and each active beam serves the user falling into its own angular coverage. $\alpha = 2.2$, $N = 16$, $K_s = 8$.

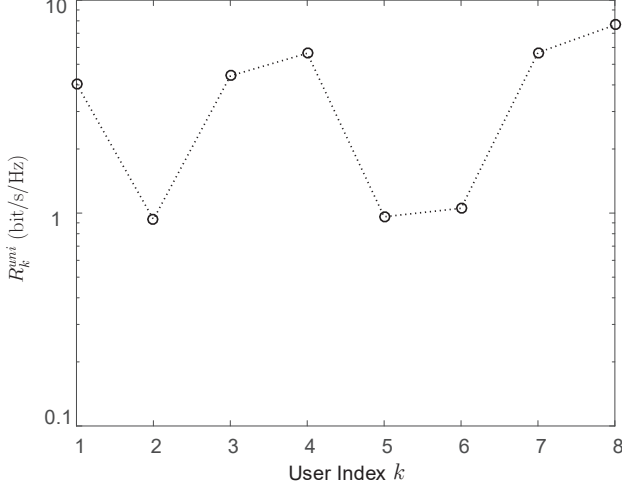


Fig. 3. Achievable data rate R_k^{uni} of each served user $k \in \mathcal{K}_s$ with LBA algorithm under the topology given in Fig. 2. The x-axis denotes the index of a user. $\alpha = 2.2$, $P_t/\sigma_0^2 = 20\text{dB}$, $N = 16$, $K_s = 8$.

A. Low-complexity Beam Allocation

To maximize the sum data rate of the system, a low-complexity beam allocation (LBA) algorithm was proposed in [8], which has been proven to be near-optimal. The LBA is a two-step algorithm: (1) each user is associated with its best beam, i.e., $n_k^{(1)} = \arg \max_{n \in \mathcal{B}} D_n(\theta_k), \forall k \in \mathcal{K}$; and (2) each associated beam is allocated to its best associated user. As the users are randomly located within the cell and have distinct angular separation from the main direction of their serving beams, it is anticipated that there are always some users locating at the edge between its serving beam and its adjacent active beam, resulting in strong interference and low data rate.

To take a close look at the individual data rates of the served users, Fig. 2 illustrates the beam allocation result by applying the LBA algorithm to a random realization of users' positions. It can be seen from Fig. 2 that there are a few "beam-edge" users. A beam-edge user is close to the angular edge between its serving beam and an adjacent beam which is active for serving another user. For example, user 2 is served by beam

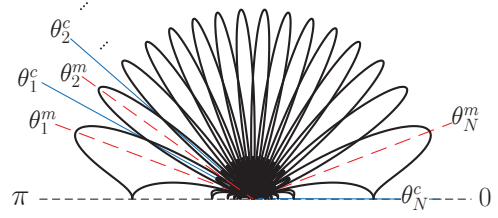


Fig. 4. Illustration of the main direction of beam n , θ_n^m , and the direction of the angular edge between beam n and beam $n+1$, θ_n^c .

2 and located at the angular edge between beam 2 and beam 3. As beam 3 is allocated to user 3 for data transmission, user 2 suffers from strong inter-beam interference from beam 3 and thus achieves low data rate which can be observed from Fig. 3. Similarly, user 5 and user 6 achieve very low data rate due to the strong inter-beam interference from each other. In this paper, these beam-edge users are referred to as *worst-case users*, which will be defined in the following subsection.

B. Definition of Worst-case Users

It is clear from the above discussion that a user $k \in \mathcal{K}_s$ is a worst-case user if two conditions are satisfied: (1) its strongest potential interfering beam is active for serving another user; and (2) it is close to the angular edge between its serving beam and strongest potential interfering beam. For the first condition, given any served user k located at (ρ_k, θ_k) , let

$$D_{n_k^{(1)}}(\theta_k) \geq D_{n_k^{(2)}}(\theta_k) \geq \dots \geq D_{n_k^{(N)}}(\theta_k) \quad (7)$$

denote the order statistics obtained by arranging the directivities $D_1(\theta_k), D_2(\theta_k), \dots, D_N(\theta_k)$ of N beams with respect to user k , where $n_k^{(l)}$ denotes the l th best beam of user k with the l th largest directivity. Particularly, beam $n_k^{(1)}$ is the beam allocated to user k for data transmission, and beam $n_k^{(2)}$ is the strongest potential interfering beam. Therefore, if a user is a worst-case user, beam $n_k^{(2)}$ must be active.

For the second condition, to quantify the closeness of a served user k to the angular edge between beam $n_k^{(1)}$ and beam $n_k^{(2)}$, let θ_n^m denote the main direction of beam n and θ_n^c denote the direction of the angular edge between beam n and beam $n+1$, as illustrated in Fig. 4. For user k , let $\theta_{n_k}^c$ denote the direction of the angular edge between its serving beam $n_k^{(1)}$ and strongest potential interfering beam $n_k^{(2)}$ where the index, \tilde{n}_k , is given by

$$\tilde{n}_k = \min\{n_k^{(1)}, n_k^{(2)}\}. \quad (8)$$

Then the closeness from user k at (ρ_k, θ_k) to the angular edge between beam $n_k^{(1)}$ and beam $n_k^{(2)}$ can be defined as

$$\Delta\psi_k = |\cos \theta_k - \cos \theta_{\tilde{n}_k}^c|. \quad (9)$$

Intuitively, a smaller $\Delta\psi_k$ indicates that user k is closer to its strongest potential interfering beam. Therefore, if a user is a worst-case user, the angular separation $\Delta\psi_k$ must be smaller than a given threshold $\Delta\psi_{th}$. To conclude, the definition of worst-case users is given as follows.

Algorithm 1 Adaptive Frequency Reuse

```

1: Input:  $\Delta\psi_{th}$ ,  $\mathcal{K}_s$ ,  $\mathcal{B}_s$ .
2: Initialization:  $\mathcal{B}_1^{adp} = \emptyset$ ,  $\mathcal{B}_2^{adp} = \emptyset$ ,  $\mathcal{B}_{full}^{adp} = \emptyset$ .
3: for  $k \in \mathcal{K}_s$  do
4:    $n_k^{(1)} = \arg \max_{n \in \mathcal{B}} D_n(\theta_k)$ ,  $n_k^{(2)} = \arg \max_{n \in \mathcal{B}, n \neq n_k^{(1)}} D_n(\theta_k)$ ;
5:   if  $n_k^{(2)} \in \mathcal{B}_s$  then
6:      $\tilde{n}_k = \min\{n_k^{(1)}, n_k^{(2)}\}$ ,  $\Delta\psi_k = |\psi_k - \psi_{\tilde{n}_k}^c|$ ;
7:     if  $\Delta\psi_k \leq \Delta\psi_{th}$  then
8:       if  $n_k^{(1)}$  is odd then
9:          $\mathcal{B}_1^{adp} = \mathcal{B}_1^{adp} \cup \{n_k^{(1)}\}$ ,  $\mathcal{B}_2^{adp} = \mathcal{B}_2^{adp} \cup \{n_k^{(2)}\}$ ;
10:      else
11:         $\mathcal{B}_2^{adp} = \mathcal{B}_2^{adp} \cup \{n_k^{(1)}\}$ ,  $\mathcal{B}_1^{adp} = \mathcal{B}_1^{adp} \cup \{n_k^{(2)}\}$ ;
12:      end if
13:    end if
14:  end for
15: end for
16:  $\mathcal{B}_{full}^{adp} = \mathcal{B}_s \setminus \mathcal{B}_1^{adp} \setminus \mathcal{B}_2^{adp}$ .
17: Output:  $\mathcal{B}_1^{adp}$ ,  $\mathcal{B}_2^{adp}$ ,  $\mathcal{B}_{full}^{adp}$ .

```

Definition 1. A user $k \in \mathcal{K}$ is a worst-case user, denoted by $k \in \mathcal{K}_{worst}$, with the following properties:

- (1) User k is served, i.e., $k \in \mathcal{K}_s$;
- (2) User k 's strongest potential interfering beam $n_k^{(2)}$ is allocated to another user for data transmission, i.e., $n_k^{(2)} \in \mathcal{B}_s$;
- (3) The angular separation from user k to the edge between beam $n_k^{(1)}$ and beam $n_k^{(2)}$, $\Delta\psi_k$, is no larger than the threshold $\Delta\psi_{th}$, i.e., $\Delta\psi_k \leq \Delta\psi_{th}$.

As the worst-case users could suffer from very strong inter-beam interference and very low data rate, we are particularly interested in improving the data rates of the worst-case users in this paper. To this end, an adaptive frequency reuse scheme will be proposed in the following section.

IV. ADAPTIVE FREQUENCY REUSE OF GREEDY BEAM ALLOCATION

A. Adaptive Frequency Reuse

As described in Section III, although the LBA algorithm can achieve near-optimal sum data rate, there could be some worst-case users who suffer from very low data rate due to strong inter-beam interference. To improve the data rates of these users, an adaptive frequency reuse scheme will be proposed in this section to allocate different frequency bands to the highly cross-interfered adjacent beams so that the interference from adjacent beams, which contributes to most of the inter-beam interference, can be eliminated. Specifically, for any worst-case user $k \in \mathcal{K}_{worst}$, to eliminate the strong inter-beam interference from beam $n_k^{(2)}$, we propose to allocate distinct half frequency bands to its serving beam $n_k^{(1)}$ and interfering beam $n_k^{(2)}$ for data transmission. Specifically, let \mathcal{B}_{half}^{adp} denote the set of the worst-case users' serving beams and strongest interfering beams, i.e., $\mathcal{B}_{half}^{adp} = \{n_k^{(1)}, n_k^{(2)} : k \in \mathcal{K}_{worst}\}$. For each beam $n \in \mathcal{B}_{half}^{adp}$, if n is odd, the first half frequency

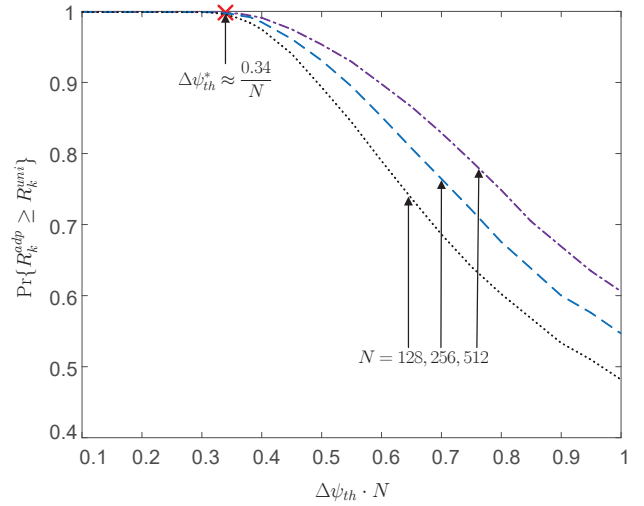


Fig. 5. Probability $\Pr\{R_k^{adp} \geq R_k^{uni}\}$ that the achievable data rate of any worst-case user $k \in \mathcal{K}_{worst}$ with the proposed adaptive frequency reuse is no less than that with universal frequency reuse versus the threshold $\Delta\psi_{th}$. $\alpha = 2.2$, $P_t/\sigma_0^2 = 20\text{dB}$, $K = 50$.

band (Subband 1) is allocated, i.e., $n \in \mathcal{B}_1^{adp}$; if n is even, the second half frequency band (Subband 2) is allocated, i.e., $n \in \mathcal{B}_2^{adp}$. For the rest of active beams, full frequency band is allocated. The corresponding beam set is denoted by \mathcal{B}_{full}^{adp} with $\mathcal{B}_{full}^{adp} = \mathcal{B}_s \setminus \mathcal{B}_{half}^{adp}$. The detailed description is presented as Algorithm 1.

With the proposed adaptive frequency reuse scheme, the achievable data rate of user k , R_k^{adp} , is given by

$$R_k^{adp} = \begin{cases} \log_2 \left(1 + \frac{P_k}{\sigma_0^2 + I_k^{adp}} \right), & \text{if } n_k^{(1)} \in \mathcal{B}_{full}^{adp}, \\ \frac{1}{2} \log_2 \left(1 + \frac{P_k}{\frac{1}{2}\sigma_0^2 + I_k^{adp}} \right), & \text{if } n_k^{(1)} \in \mathcal{B}_i^{adp}, i = 1, 2. \end{cases} \quad (13)$$

For any user k , if its allocated beam $n_k^{(1)}$ transmits over the whole frequency band, it receives the whole inter-beam interference from all the active beams. If $n_k^{(1)}$ transmits over subband i , it receives the whole interference from the beams working on the same subband i and half of the interference from the beams working on the full frequency band. Therefore, the inter-beam interference power received at user k , I_k^{adp} , can be obtained as (12) shown at the top of this page.

As whether a user is a worst-case user closely depends on the threshold $\Delta\psi_{th}$, the adaptive frequency band allocation result is determined by the threshold $\Delta\psi_{th}$. Specifically, with a small $\Delta\psi_{th}$, some users close to the strongest interfering beams may not be included into the worst-case user set and thus full frequency band is allocated which results in strong inter-beam interference and low data rate. While $\Delta\psi_{th}$ is large, some users relatively far away from their strongest interfering beams may be labeled as worst-case users with half frequency band allocated which results in low data rate as well. Therefore, the threshold $\Delta\psi_{th}$ needs to be carefully chosen for improving the individual data rate.

$$I_k^{adp} = \begin{cases} \sum_{n \in \mathcal{B}_s, n \neq n_k^{(1)}} p_n \cdot D_n(\theta_k) \cdot \rho_k^{-\alpha}, & \text{if } n_k^{(1)} \in \mathcal{B}_{full}^{adp}, \\ \sum_{n \in \mathcal{B}_i^{adp}, n \neq n_k^{(1)}} p_n \cdot D_n(\theta_k) \cdot \rho_k^{-\alpha} + \frac{1}{2} \sum_{n \in \mathcal{B}_{full}^{adp}} p_n \cdot D_n(\theta_k) \cdot \rho_k^{-\alpha}, & \text{if } n_k^{(1)} \in \mathcal{B}_i^{adp}, i = 1, 2. \end{cases} \quad (12)$$

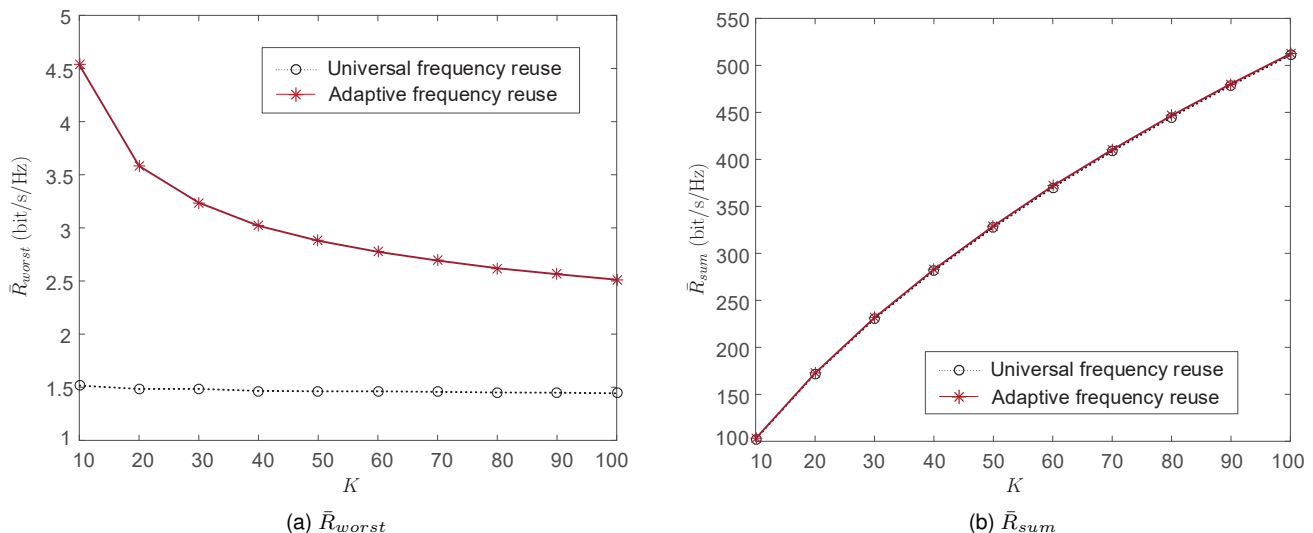


Fig. 6. (a) Average data rate per worst-case user \bar{R}_{worst} and (b) average sum data rate \bar{R}_{sum} with the proposed adaptive frequency reuse and universal frequency reuse. $\alpha = 2.2$, $\bar{P}_t/\sigma_0^2 = 20\text{dB}$, $N = 512$.

As we aim at improving the achievable data rates of the low-data-rate users with universal frequency reuse by adopting the proposed adaptive frequency reuse algorithm, all the users who can achieve higher data rate by using half frequency band than by using full frequency band should be included in the worst-case user set \mathcal{K}_{worst} . As a result, the threshold $\Delta\psi_{th}$ should be maximized as far as possible. Fig. 5 presents the probability $\Pr\{R_k^{adp} \geq R_k^{uni}\}$ that the achievable data rate of any worst-case user $k \in \mathcal{K}_{worst}$ with adaptive frequency reuse is no less than that with universal frequency reuse. It can be seen from Fig. 5 that with a small threshold $\Delta\psi_{th}$, the probability $\Pr\{R_k^{adp} \geq R_k^{uni}\}$ is 1, implying that all the worst-case users achieve higher data rate by using adaptive frequency reuse. As $\Delta\psi_{th}$ increases, $\Pr\{R_k^{adp} \geq R_k^{uni}\}$ decreases rapidly which indicates that some users who can achieve higher data rate by using full frequency band instead of half frequency band are included in the worst-case user set. Therefore, to improve the individual data rate by adopting adaptive frequency reuse, the threshold $\Delta\psi_{th}$ should be properly chosen, and the threshold should be maximized as much as possible under the constraint that $\Pr\{R_k^{adp} \geq R_k^{uni}\} = 1$. It can be seen that the optimal threshold $\Delta\psi_{th}^*$ is $0.34/N$, which solely determined by the number of beams N .

B. Simulation Results

Fig. 6 presents the average achievable data rate per worst-case user $\bar{R}_{worst} \triangleq \mathbb{E}_{\{\mathbf{r}_k: k \in \mathcal{K}\}} [R_k | k \in \mathcal{K}_{worst}]$ and the average sum data rate $\bar{R}_{sum} \triangleq \mathbb{E}_{\{\mathbf{r}_k: k \in \mathcal{K}\}} [\sum_{k \in \mathcal{K}_s} R_k]$ under varying number of users K . It can be seen in Fig. 6(a) that with

universal frequency reuse, the average data rate per worst-case user \bar{R}_{worst}^{uni} remains as a constant as the number of users K increases. The reason is that with universal frequency reuse, the strongest adjacent interfering beam of each worst-case user is allocated with the same frequency band, which contributes to most of the worst-case user's inter-beam interference. As a result, by increasing the number of users K , although the total number of active beams increases, the inter-beam interference suffered by each worst-case user is almost a constant and thus the average data rate per worst-case user \bar{R}_{worst}^{uni} is independent of the number of users K .

If adaptive frequency reuse is applied, the strongest interfering beam of a worst-case user is allocated with distinct half frequency band, resulting in no inter-beam interference for the worst-case user. That is, a worst-case user only suffers from inter-beam interference from other active beams. Since the number of served users/active beams K_s in the system increases with the number of users K , the inter-beam interference increases accordingly. As a result, \bar{R}_{worst}^{adp} decreases as K increases. It can be clearly seen from Fig. 6 that the proposed adaptive frequency reuse can greatly improve the average data rate per worst-case user while maintaining similar average sum data rate to that with universal frequency reuse.

V. CONCLUSION

In this paper, an adaptive frequency reuse scheme has been proposed to mitigate the severe inter-beam interference and improve the data rates of the worst-case users in a beam allocation based multiuser massive MIMO system. Simulation

results have shown that the proposed adaptive frequency reuse can increase the worst-case users' data rates greatly while achieving similar sum data rate to universal frequency reuse, implying that the fairness among the served users can be improved by adopting our proposed adaptive frequency reuse scheme. In addition, with our proposed adaptive frequency reuse scheme, the frequency band allocations for different users are independent from each other. As a result, frequency bands can be allocated to users in parallel, indicating that our proposed adaptive frequency reuse scheme can be easily adopted in future beam allocation based multiuser massive MIMO systems.

ACKNOWLEDGMENT

This work is currently supported by the UK Engineering and Physical Sciences Research Council, project EP/L026031/1, NIRVANA. It was also partly carried out within the framework of the EU-Japan Horizon 2020 Research and Innovation Programme, grant agreement no. 643297 (RAPID).

REFERENCES

- [1] J. G. Andrews, S. Buzzi, W. Choi, S. V. Hanly, A. Lozano, A. C. K. Soong, and J. C. Zhang, "What will 5G be?" *IEEE J. Select. Areas Commun.*, vol. 32, no. 6, pp. 1065–1082, June 2014.
- [2] A. Lozano and A. M. Tulino, "Capacity of multiple-transmit multiple-receive antenna architectures," *IEEE Trans. Inf. Theory*, vol. 48, no. 12, pp. 3117–3128, Dec. 2002.
- [3] T. L. Marzetta, "Noncooperative cellular wireless with unlimited numbers of base station antennas," *IEEE Trans. Wireless Commun.*, vol. 9, no. 11, pp. 3590–3600, Nov. 2010.
- [4] F. Rusek, D. Persson, B. K. Lau, E. G. Larsson, T. L. Marzetta, O. Edfors, and F. Tufvesson, "Scaling up MIMO: Opportunities and challenges with very large arrays," *IEEE Signal Process. Mag.*, vol. 30, no. 1, pp. 40–60, Jan. 2013.
- [5] V. Venkateswaran and A. Veen, "Analog beamforming in MIMO communications with phase shift networks and online channel estimation," *IEEE Trans. Signal Process.*, vol. 58, no. 8, pp. 4131–4143, Aug. 2010.
- [6] O. N. Alrabadi, E. Tsakalaki, H. Huang, and G. F. Pedersen, "Beamforming via large and dense antenna arrays above a clutter," *IEEE J. Select. Areas Commun.*, vol. 31, no. 2, pp. 314–325, Feb. 2013.
- [7] S. Hur, T. Kim, D. J. Love, J. V. Krogmeier, T. A. Thomas, and A. Ghosh, "Millimeter wave beamforming for wireless backhaul and access in small cell networks," *IEEE Trans. Commun.*, vol. 61, no. 10, pp. 4391–4403, Oct. 2013.
- [8] J. Wang, H. Zhu, L. Dai, N. J. Gomes, and J. Wang, "Low-complexity beam allocation for switched-beam based multiuser massive MIMO systems," *IEEE Trans. Wireless Commun.*, vol. 15, no. 12, pp. 8236–8248, Dec. 2016.
- [9] J. Brady and A. Sayeed, "Beamspace MU-MIMO for high-density gigabit small cell access at millimeter-wave frequencies," in *Proc. IEEE SPAWC*, pp. 80–84, June 2014.
- [10] P. Amadori and C. Masouros, "Low RF-complexity millimeter-wave beamspace-MIMO systems by beam selection," *IEEE Trans. Wireless Commun.*, vol. 63, no. 6, pp. 2212–2223, June 2015.
- [11] J. Hogan and A. Sayeed, "Beam selection for performance-complexity optimization in high-dimensional MIMO systems," in *Proc. CISS*, pp. 337–342, Mar. 2016.
- [12] X. Gao, L. Dai, Z. Chen, Z. Wang, and Z. Zhang, "Near-optimal beam selection for beamspace mmWave massive MIMO systems," *IEEE Commun. Letters*, vol. 20, no. 5, pp. 1054–1057, May 2016.
- [13] O. E. Ayach, S. Rajagopal, S. Abu-Surra, Z. Pi, and R. W. Heath, "Spatially sparse precoding in millimeter wave MIMO systems," *IEEE Trans. Wireless Commun.*, vol. 13, no. 3, pp. 1499–1513, Mar. 2014.
- [14] T. E. Bogale, L. B. Le, A. Haghghat, and L. Vandendorpe, "On the number of RF chains and phase shifters, and scheduling design with hybrid analog-digital beamforming," *IEEE Trans. Wireless Commun.*, vol. 15, no. 5, pp. 3311–3326, May 2016.
- [15] M. N. Kulkarni, A. Ghosh, and J. G. Andrews, "A comparison of MIMO techniques in downlink millimeter wave cellular networks with hybrid beamforming," *IEEE Trans. Commun.*, vol. 64, no. 5, pp. 1952–1967, May 2016.
- [16] J. Butler and R. Lowe, "Beam-forming matrix simplifies design of electrically scanned antennas," *Electronic Design*, Apr. 1962.
- [17] M. R. Akdeniz, Y. Liu, M. K. Samimi, S. Sun, S. Rangan, T. S. Rappaport, and E. Erkip, "Millimeter wave channel modeling and cellular capacity evaluation," *IEEE J. Select. Areas Commun.*, vol. 32, no. 6, pp. 1164–1179, June 2014.